

Article

Performance of Thermal-, Acid-, and Mechanochemical-Activated Montmorillonite for Environmental Protection from Radionuclides U(VI) and Sr(II)

Iryna Kovalchuk ^{1,2} 

¹ Institute for Sorption and Problems of Endoecology, National Academy of Science of Ukraine, 03164 Kyiv, Ukraine; kovalchukiryna@gmail.com

² Department of Chemical Technology of Ceramics and Glass, National Technical University of Ukraine "Igor Sikorsky Kyiv Polytechnic Institute", 03056 Kyiv, Ukraine

Abstract: Low-cost sorption materials based on the clay mineral of the smectite group—montmorillonite—were used for the removal of radionuclides uranium (VI) and strontium (II) from contaminated water. A wide range of industrial methods such as thermal treatment, acid activation, and mechanochemical activation were applied. Complex methods, such as SEM microscopy analysis, X-ray powder diffraction (XRD), thermal analysis, and nitrogen adsorption–desorption at -196°C , were used to assess the characteristics of the structure of the obtained materials. The thermal treatment, acid activation, and mechanochemical activation resulted in changes in the surface properties of the clay minerals: specific surface area, porosity, and distribution of active sites. It was established that the mechanochemical activation of montmorillonite significantly increases the sorption characteristics of the material for U(VI) and Sr(II) and the acid activation of montmorillonite increases it for U(VI). The appropriateness of the experimental adsorption values for U(VI) and Sr(II) on modified montmorillonite to Langmuir and Freundlich models was found. Independently of the changes induced by acid attack, calcinations, or milling, the sorption of U(VI) and Sr(II) ions on treated montmorillonite occurs on a homogeneous surface through monolayer adsorption in a similar fashion to natural montmorillonite. Water purification technologies and modern environmental protection technologies may successfully use the obtained clay-based sorbents.

Keywords: montmorillonite; clay treatment; radionuclides; adsorption; water removal



Citation: Kovalchuk, I. Performance of Thermal-, Acid-, and Mechanochemical-Activated Montmorillonite for Environmental Protection from Radionuclides U(VI) and Sr(II). *Eng* **2023**, *4*, 2141–2152. <https://doi.org/10.3390/eng4030122>

Academic Editor: Antonio Gil Bravo

Received: 29 June 2023

Revised: 20 July 2023

Accepted: 9 August 2023

Published: 11 August 2023



Copyright: © 2023 by the author. Licensee MDPI, Basel, Switzerland. This article is an open access article distributed under the terms and conditions of the Creative Commons Attribution (CC BY) license (<https://creativecommons.org/licenses/by/4.0/>).

1. Introduction

The uranium mining and uranium processing industry leads to the pollution of environmental uranium compounds [1]. Radioactive waste disposal sites from the blocked waters of the radioactive sites of nuclear power plants, and nuclear power plant accidents are a potential source of radionuclides in water areas [2]. The decommissioning of several industrial enterprises and the formation of a significant amount of dangerous pollutants has taken place as a result of the war in Ukraine. Military weapon strikes damage the sites of extraction, processing, storage, and disposal of radioactive substances.

In addition, damage caused by military weapons leads to the release of toxic and radioactive substances into the environment as a result of explosions. Radioactive elements enter drinking water sources and they are a threat to public health. According to the World Health Organization, the maximum allowable limit in water for uranium consists of 0.03 mg/L, and for strontium-90, it consists of 2.0 Bq/L. The total beta activity for drinking water consists of ≤ 1.0 Bq/L [3]. Therefore, the high level of inorganic pollutants in the water is a significant ecological problem and needs a practical solution for sphere environmental protection.

Taking into account the very large areas with contaminated water and the huge volumes of waste generated during the mining and processing of radioactive ores, it

becomes especially important to search for the cheapest reagents and materials used in appropriate environmental protection technologies [4,5].

Among the different methods for the purification of contaminated waters, sorption has an advantage because the selective removal of small amounts of toxicants can occur. Today, a wide variety of natural and synthetic sorbents are offered for water purification [6,7]. However, the feasibility of using natural clay minerals is due to their availability and low cost.

Clay mineral montmorillonite is the main representative of the smectite group. The base structural unit of montmorillonite comprises two tetrahedrally coordinated sheets of silicon ions surrounding octahedrally coordinated sheets of aluminum ions (2:1 type). As a result of the isomorphous substitution of Si^{4+} for Al^{3+} in the tetrahedral layer and Al^{3+} for Mg^{2+} in the octahedral layer, a net negative surface charge on the clay occurs [8]. These structure characteristics conduct the excellent sorption properties of montmorillonite, which possesses available sorption sites at the basal surface, edge sites, and within its interlayer space [9–11]. For the removal of Co, Cu, Zn, Cd, and U, montmorillonite was used [12,13]. The large adsorption capacity of montmorillonite for these metals was proved. Uranium (VI) sorption onto bentonite colloids in carbonate-containing groundwater was investigated [14,15]. The removal of Sr^{2+} ions from contaminated water was investigated [16].

The physical and chemical modification of the surface of clay minerals makes it possible to significantly improve their sorption and technological characteristics. Various methods of physical and chemical surface modification to increase the sorption capacity of layered silicates with the aim of their further use in industries have been widely used [17,18]. The most common are acid [19], mechanochemical activation [20], hydrothermal treatment, thermal activation [21], surface modification with organic substances [22], obtaining pillared clay minerals [23], surface modification with nano-dispersed metal powders [24,25], and chemical grafting on the surface of complex compounds [26], among other methods [27,28].

In industrial applications using clays as sorbent materials, one of the simplest technological operations to increase their surface activity is acid activation. At the same time, the cheap mineral acids HCl and H_2SO_4 are used as reagents [19,29]. An important result of the acid treatment of clay minerals (from the point of view of their further use in catalysis and sorption technologies) is the development of their meso- and microporous structure [19]. As a result of treatment with acids, first of all, the octahedral networks of layered silicates are destroyed. The final product, under harsh processing conditions (high acid concentration, processing temperature) and the sufficient duration of the process, is always highly porous amorphous silica [19,30]. The effect of the acid treatment on the clay structure is that it opens up the edges of the platelets. Therefore, the diameter of the pores and the surface area increases. The acid-modified clays have been found particularly useful for the adsorption of As, Cd, Cr, Co, Cu, Fe, Pb, Mn, Ni, and Zn in their ionic forms from an aqueous medium [10,31,32].

Fine dispersion is one of the main technological operations in the silicate industry and in the processing of mineral raw materials. The development and application of energy-intensive units (disintegrators, centrifugal-planetary mills, etc.) in the process of grinding solids not only ensures the achievement of the high dispersion of the final products but also, to a large extent, influences the concentration and nature of surface defects [33–35]. This circumstance provides broad prospects for the application of mechanochemical activation in catalyst technology and sorption processes [36,37]. The mechanochemical treatment appeared to decrease the structure order and increase the specific surface area of the clays. These phenomena: fragmentation, abrasion, and the amorphization of the particles lead to a higher cation exchange capacity and thus to an improved sorption capability [38]. Mechanochemically treated montmorillonite and kaolinite proved to be effective sorbents for the removal of heavy metals [39].

Along with milling processes, thermal treatment at different temperatures (drying, dehydroxylation, annealing) is one of the key operations in silicate technology. Drying processes usually include the loss of mechanically trapped, capillary, and adsorption-bound water and occur in a range of up to 200 °C. The dehydroxylation of clay minerals, which

is accompanied by a partial restructuring of the structure, takes place in the temperature range of 400–700 °C. During annealing, a deep restructuring of the mineral structure occurs with the formation of new amorphous and crystalline phases [21,40]. The thermal dehydration of montmorillonite is accompanied by a decrease in its interplanar distance, as well as a partial decrease in its cation-exchange capacity. Water, removed from the structure of montmorillonite when heated, frees the pore space, thereby increasing the textural characteristics of the mineral [41]. The calcination of montmorillonite leads to the loss of the ability of the mineral structure to interlayer swelling and, thus, a decrease in the size of the active surface that participates in ion exchange. As a result, the amount of sorbed cobalt is decreased [42].

The applications of thermally modified and acid-activated clay minerals for environmental protection were demonstrated [43]. Contaminants such as pesticides, heavy metals, dyes, benzene, toluene, ethyl-benzene, xylenes, and methyl tertiary butyl ether were removed to a highly efficient degree.

The objective of the present study is the removal of U(VI) and Sr(II) from contaminated water by the sorption on thermal-, acid-, and mechanochemical-treated montmorillonite. X-ray diffraction, scanning electron microscopy, and low-temperature N₂ adsorption were used to explain the structure and surface morphology of the sorbents after the treatment of the montmorillonite. The mechanism of the sorption removal of these radionuclides from water was found.

2. Materials and Methods

2.1. Materials and Chemicals

Montmorillonite (MMT) is the mineral of the smectite group (2:1 type). MMT was taken from the Cherkasy bentonite deposit (Dashukivka site), PJSC “Dashukiv Bentonites”, Lysyanka city, Cherkasy region, Ukraine. Its structural formula is $(Ca_{0.12}Na_{0.03}K_{0.03})_{0.18}(Al_{1.39}Mg_{0.13}Fe_{0.44})_{1.96}(Si_{3.88}Al_{0.12})_{4.0}O_{10}(OH)_2 \cdot nH_2O$ and the cation exchange capacity is 1.0 mmol/g.

Sedimentation from aqueous clay suspension and subsequent centrifugation of montmorillonite was carried out to purify coarse mineral impurities (quartz, feldspars, carbonates, aluminum, iron oxides, etc.). The obtained material was dried at 105 °C, and ground. The fraction < 0.1 mm was used for the following modification.

Hydrochloric acid (HCl), nitric acid (HNO₃), sodium hydroxide (NaOH), Arsenazo III and salts of sodium chloride (NaCl), uranyl sulfate (UO₂SO₄·3H₂O), and strontium chloride (SrCl₂·6H₂O) were obtained from Sigma–Aldrich, Burlington, MA, USA. All the chemicals were of analytical reagent grade and used without further purification. Distilled water was used for all experiments for the preparation of various concentrations of solutions.

2.2. Preparation of the Samples of Treated Montmorillonite

The natural montmorillonite has been treated in thermal, acid, and mechanochemical ways demonstrated in Figure 1.

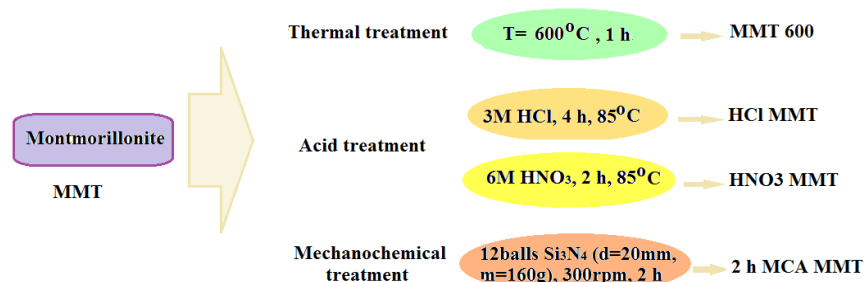


Figure 1. Diagram of the experiment of the thermal, acid, and mechanochemical montmorillonite treatment.

Thermal treatment of samples of natural MMT consisted of calcining the samples in the air in a muffle furnace SNOL 8.2/1100 (SnolTherm, UAB, Narkūnai, Lithuania) at 600 °C for 1 h.

Acid activation of the surface of MMT was carried out in solutions of 3 M and 6 M nitric (HNO₃)/hydrochloric (HCl) acids at 2 and 4 h without heating/at 85 °C with constant stirring using a magnetic stirrer. The clay mineral acid ratio was 1:4. After the synthesis, the samples were washed with distilled water from acid to negative reaction onto chlorides/nitrates.

Mechanochemical activation of MMT was carried out using planetary ball mill Pulverisette-6 (Fritsch, Idar-Oberstein, Germany) with a rotation speed of 300 rpm. The diameter of the Si₃N₄ balls was 20 mm, and the total weight was 160 g. The mass ratio of the balls/sample consists of about 10. Milling was performed in 10 min cycles; subsequently, a reverse was carried out after each cycle. The duration of milling was 2 h.

2.3. Characterization of Samples

Thermogravimetric analysis was performed on F. Paulik, J. Paulic, L. Erdey derivatograph (Hungary) in a temperature range of 20–1000 °C at a heating rate of 10 min⁻¹.

X-ray powder diffraction (XRD) of the natural clay mineral and thermal-, acid-, and mechanochemically activated MMT were recorded on DRON-4-07 diffractometer (SPE Burevestnik, Nizhniy Novgorod, Russia) under the following conditions: range of 2–60° (2θ) using CuKα radiation, λ = 0.154 nm, and were acquired at constant pass energy of U = 30 kV, I = 30 mA [44].

The surface morphology of montmorillonite samples was investigated using SEM method on Jeol JSM-6060 (Tokyo, Japan) scanning electron microscope in secondary electron mode with an accelerating voltage (AV) of 30 kV. The samples were sputter coated with gold for 3 min.

Low-temperature nitrogen adsorption isotherms were determined on a volumetric automatic apparatus (Quantachrome, Nova 2200e Surface Area and Pore Size Analyzer, Boynton Beach, FL, USA) at –196 °C. Parameters of the porous structure of montmorillonite samples such as specific surface area (S_{BET}, m²/g), total pore volume (V, cm³/g), average pore radius (r, nm), and distribution of pore sizes of the natural and treated montmorillonite were determined using BJH and DFT methods [45].

2.4. Adsorption Experiments

The solutions prepared from salts of uranyl sulfate (UO₂SO₄·3H₂O) and strontium chloride (SrCl₂·6H₂O) were used in the sorption experiments for the removing of uranium (VI) and strontium (II) ions from water. The 0.01 M ionic strength was created with a solution of NaCl. Solutions of 0.1 M NaOH and HCl were used for pH adjustment on the Ionomer II-160MII. Sorption isotherms were obtained at pH 6.

The batch sorption experiments (the mass of sorbents 0.1 g; the volume of the aqueous phase 50 mL) were carried out in a thermostated cell (Environmental shaker ES-20, SIA Biosan, Riga, Latvia) during 1 h continuous shaking at 25 °C.

After establishing the adsorption equilibrium, the separation of the liquid phase from the solid one occurred following centrifugation at 6000 rpm for 30 min. The equilibrium uranium (VI) concentration was determined using spectrophotometrical method on instrument UNICO 2100UV (United Products and Instruments, Suite E Dayton, NJ, USA) with Arsenazo III as reagent at a wavelength of 665 nm. The atomic adsorption spectroscopy method on the AA-6300 Shimadzu, Shimadzu Corporation, Tokyo, Japan, instrument was used for Sr(II) determination of the solution. The sorption U(VI) and Sr(II) q, μmol/g, was calculated by Equation (1):

$$q = (C_{in} - C_{eq}) \times V/m, \quad (1)$$

where C_{in}, C_{eq}—the initial and equilibrium concentration of the metal, μmol/L; V—a volume of solution, L; m—a mass of the sample of sorbent, g. All experiments were undertaken in triplicate. The processing of the experimental isotherms of radionuclide

adsorption was carried out using the Langmuir mathematical model for a homogeneous surface [46] and the Freundlich model for a heterogeneous surface [47].

3. Results

The sample of thermal-treated MMT (MMT 600) was used for comparison with the ones obtained by another method of treatment [42]. The acid-activated samples (HNO_3 MMT) (6 M HNO_3 , 2 h, 85 °C) and (HCl MMT) (3 M HCl, 4 h, 85 °C) demonstrated better surface and sorption characteristics [48]. The sample with better surface and sorption characteristics was obtained after mechanochemical activation of 2 h [48].

The number of water molecules in the interlayer of MMT decreases at temperatures from 25 °C to 200 °C, the interlayer spacing decreases, the interlayers become highly ordered, and the crystal structure becomes more ordered [40]. The interlayer structure of the MMT collapses at 500–700 °C. The decomposition of the MMT unstable components (silica-alumina oxide crystals) leads to the collapse of the crystal layer (Figure 2).

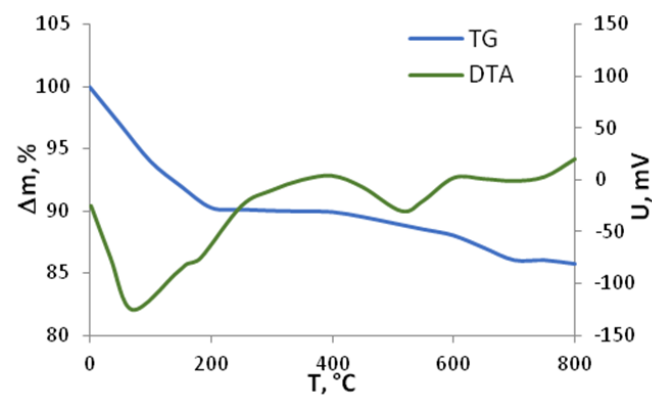


Figure 2. Thermogravimetry (TG) of natural montmorillonite.

Figure 3 shows the comparison of the X-ray diffraction patterns of the MMT, thermal-treated montmorillonite (MMT 600), acid-treated montmorillonite (HNO_3 MMT and HCl MMT), and mechanochemical-treated montmorillonite (2 h MCA MMT).

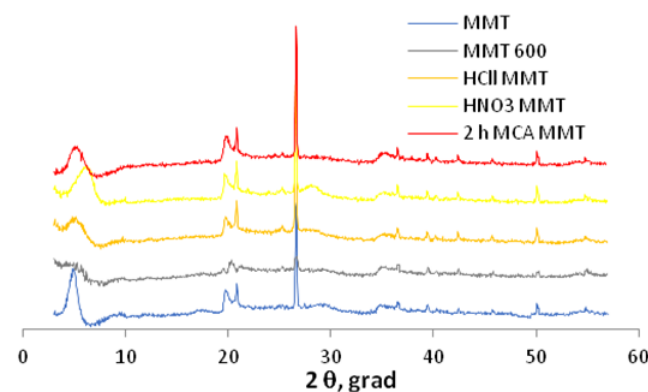


Figure 3. X-ray diffraction of natural and thermal-, acid-, and mechanochemical-treated montmorillonite.

During the thermal, acidic, and milling processes, structural changes occurred. The degree of crystallinity in the samples decreased. This was evidenced by a progressive decrease in the XRD reflection intensities: d_{001} were 1.824 nm for MMT and 1.724, 1.501, and 1.766 nm for HNO_3 MMT, HCl MMT, and 2 h MCA MMT, respectively. The broadening of the XRD reflections (Figure 3) indicated that, along with structural changes, a reduction in particle size occurred. In particular, the amorphization of structure MMT 600 occurred (Figure 3, curve 2). The mechanochemical treatment (2 h MCA MMT), similar to acid one (HNO_3 MMT, HCl MMT), led to the decrease in the intensity of the 001 peak and the shift of

the 001 peak, with concomitant broadening in an asymmetrical fashion. This indicates that the stacking of the layers was disrupted and lost, and the initial structural destabilization of the basal plane began [29,34,36].

The morphology of the natural (MMT) and different treatment methods of the montmorillonite samples (MMT 600, HNO₃ MMT, 2 h MCA MMT) was observed by using high-resolution SEM. The morphology of the natural MMT consisted of the platy clay particles (Figure 4a). For the series of montmorillonite samples, the microstructure changed with the treatment performed (Figure 4b–d). The thermal treatment changed the structure of the MMT (Figure 4b); there was a more significant decrease in particles' size in the MMT 600 sample. The acid activation of the MMT led to the loosening of the edges of the mineral structure (HNO₃ MMT) and the formation of flaky edges (Figure 4c). Contrary to natural MMT, the morphology of the mechanochemically activated sample (MCA MMT 2 h) was more uniform and was dominated by spherulitic and (quasi-)regular particles. In the results of the mechanochemical treatment, flaky edges appeared (Figure 4d).

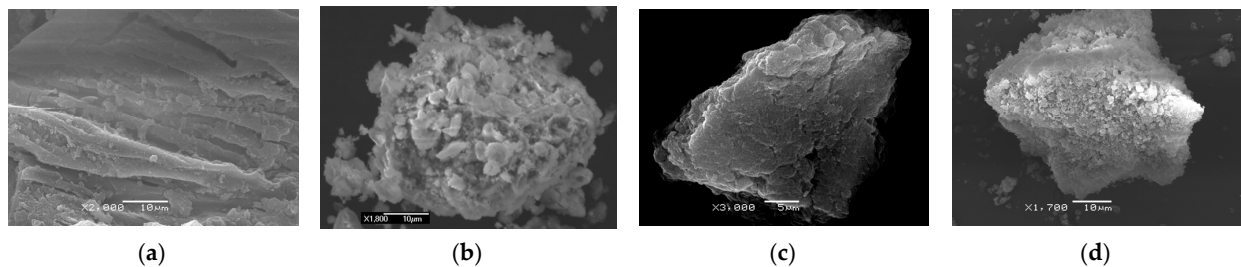


Figure 4. SEM microphotographs of the particles of natural (a) and thermal- (b), acid- (c), and mechanochemical- (d) treated montmorillonite.

The nitrogen sorption–desorption isotherm (Figure 5a) on the natural montmorillonite, according to the IUPAC classification, is attributed to type II [45]. The nitrogen adsorption curves of the MMT are similar to those on the samples of MMT 600, HNO₃ MMT, HCl MMT, and 2 h MCA MMT. This is typical for nonporous sorbents with a small macroporous component. The isotherms MMT, MMT 600, HNO₃ MMT, HCl MMT, and 2 h MCA MMT in the range of values $p/p_0 > 0.4$ have the hysteresis loops of the H3 type, indicating a well-developed structure with slit-like pores [49,50].

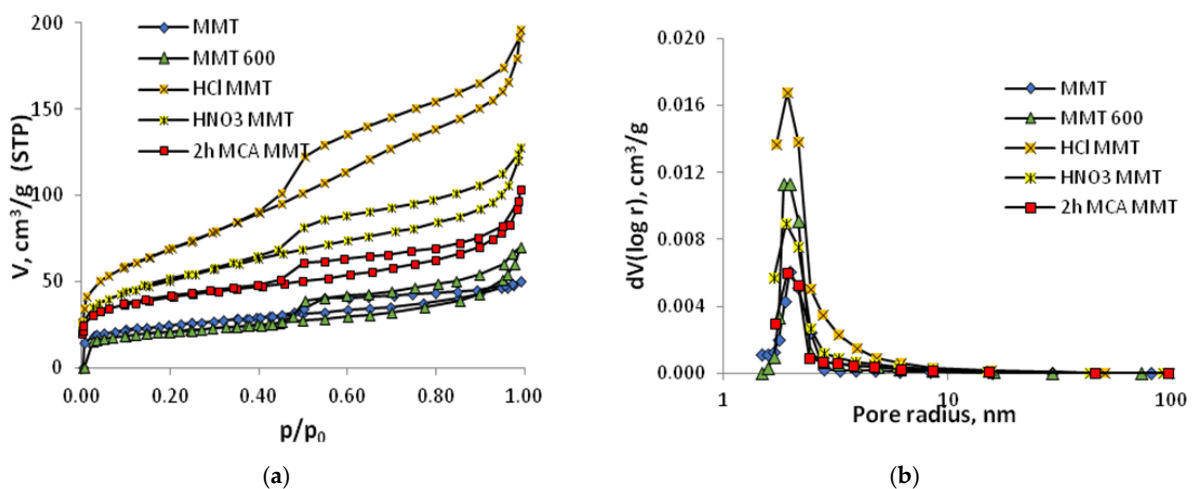


Figure 5. Nitrogen adsorption–desorption isotherms (a) and differential size distribution curves of the pores (BJH method) (b) of natural and thermal-, acid-, and mechanochemical-treated montmorillonite.

The mesopore-size distributions (Figure 5b) from the low-temperature nitrogen adsorption data were calculated using the currently used Barrett–Joyner–Halenda (BJH) method [45].

The maximum in the pore-size distribution of the natural montmorillonite was centered at 1.98 nm (Figure 5). This value slightly decreased after treatment to 1.87 ÷ 1.93 nm. The narrow peaks ($r = 1.5 \div 3.0$ nm) in the montmorillonite samples indicated narrow pore volume distribution by size. The calculations of the nitrogen isotherm-based characteristics of the porous structure presented in Table 1 indicated that the specific surface area of the samples, determined using the BET method, increased after the surface modification. The specific surface area (S_{BET}) of the MMT (89.1 m^2/g) increased after the surface modification and consisted of 179.4 and 244.0 m^2/g for HNO_3 MMT and HCl MMT, respectively, and 146.8 m^2/g for 2 h MCA MMT. The insignificant decreasing surface area of the MMT for the thermally treated mineral MMT 600 occurred to 75.4 m^2/g (Table 1).

Table 1. Surface characteristics of natural and thermal-, acid-, and mechanochemical-treated montmorillonite.

Sample	S, m^2/g	V, cm^3/g	r, nm	Distribution of Pore Sizes, nm				
				BJH $dV(r)$		DFT $dV(r)$		
				r ₁	r ₂	r ₁	r ₂	r ₃
MMT	89.1	0.078	1.753	1.98	-	1.41	2.75	-
MMT 600	75.4	0.108	2.867	1.87	-	0.83	2.59	-
HNO_3 MMT	179.4	0.198	2.213	1.91	-	1.25	2.54	0.69
HCl MMT	244.0	0.304	2.500	1.93	-	0.72	2.64	-
2 h MCA MMT	146.8	0.161	2.187	1.92	-	1.13	2.64	0.67

The sorption isotherms of the uranium ions indicate a significant influence of the treatment using different methods on the sorption magnitude (Figure 6a). The obtained sorption characteristics for strontium ions in the modified samples of montmorillonite (Figure 6b) were changed to high values for the mechanochemical-activated MMT only. Langmuir and Freundlich models were used to estimate the adsorption capacity of the natural and treated montmorillonite. The obtained data are presented in Table 2.

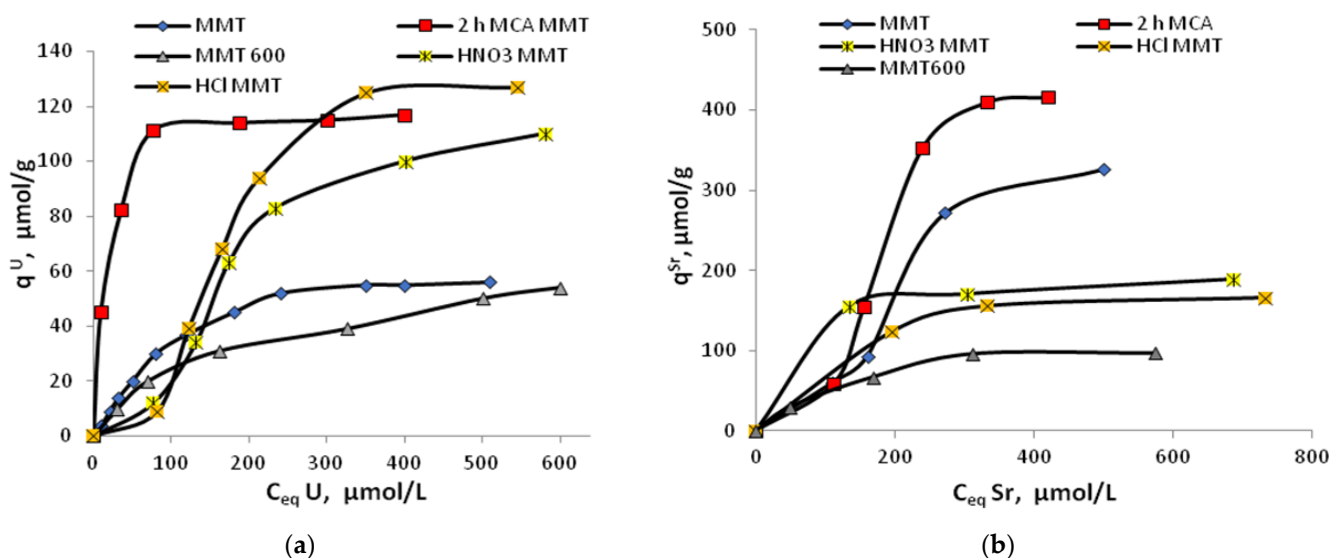


Figure 6. Isotherms of sorption of U(VI) (a) and Sr(II) (b) by the natural and thermal-, acid-, and mechanochemical-treated montmorillonite.

Table 2. Langmuir and Freundlich parameters for the adsorption of uranyl and strontium ions onto natural and thermal-, acid-, and mechanochemical-treated montmorillonite.

Me	Sample	Langmuir			Freundlich		
		$q_m, \mu\text{mol g}^{-1}$	$K_L, \text{L } \mu\text{mol}^{-1}$	R^2	n^{-1}	$K_F, \text{L } \mu\text{mol}^{-1}$	R^2
U(VI)	MMT	67.6	0.048	0.994	0.90	1.189	0.988
	MMT 600	55.0	0.032	0.997	0.57	3.911	0.992
	HCl MMT	161.3	0.033	0.973	0.75	1.040	0.829
	HNO ₃ MMT	140.9	0.025	0.999	0.70	0.776	0.818
	2 h MCA MMT	120.5	0.349	0.999	0.25	0.692	0.844
Sr(II)	MMT	434.8	0.024	0.999	1.19	3.786	0.914
	MMT 600	163.9	0.018	0.990	0.51	0.630	0.931
	HCl MMT	185.2	0.045	0.996	0.21	0.767	0.828
	HNO ₃ MMT	200.0	0.105	0.999	0.12	0.830	0.999
	2 h MCA MMT	555.6	0.038	0.982	1.47	8.335	0.878

q_m —the amount of adsorbate corresponding to complete monolayer coverage; K_L —Langmuir bonding energy coefficient; K_F —Freundlich coefficient of adsorption capacity; n —coefficient of adsorption intensity; R —correlation coefficient.

The Langmuir model better agrees with the experimental data, as evidenced by the higher correlation coefficient values ($R^2 = 0.973 \div 0.999$) compared with the Freundlich model ($R^2 = 0.818 \div 0.999$). The equation of monomolecular Langmuir sorption assumes the energy homogeneity of the active centers and, accordingly, the ion sorption energies close as the surface fills. The empirical Freundlich equation is suitable mainly for describing the beginning areas of isotherms. The value of K_F is associated with the interaction energy between the adsorbent and the adsorbate. The higher values of K_F indicate stronger interactions and mean a greater affinity or possible selectivity.

4. Discussion

There are two main types of active sites situated on the surface of layer silicates where the sorption of metal ions takes place. The first one is the exchange cations localized on the basal surfaces of the particles, the appearance of which is conditioned by the nonstoichiometric isomorphous substitutions in the tetrahedral and octahedral sheets of the structural layers. The second one is the Si–OH and Al–OH groups that are situated on the side edges of the particles at the place of disrupted Si–O–Si- and Al–O–Al-structured sheets.

The uranium uptake of the studied samples of montmorillonite is quite a complicated phenomenon associated with the aqueous chemistry of the elements and the nature of the materials. The chemical form of uranium in water is one of the main conditions that define its adsorption on natural minerals. In aqueous solutions, the uranium (VI) ions characteristically form a different complex at indicated pH values. In natural water, at pH near neutral values, uranium (VI) can exist in the form of a series of mono- and poly-nuclear hydroxo-complexes, such as UO_2^{2+} , UO_2OH^+ , $(\text{UO}_2)_2(\text{OH})_2^{2+}$, $(\text{UO}_2)_3(\text{OH})_4^{2+}$, $(\text{UO}_2)_3(\text{OH})_5^+$, $(\text{UO}_2)_4(\text{OH})_7^+$, and others. In groundwater, the contents of neutral and negatively charged forms $\text{UO}_2(\text{OH})_2$, UO_2CO_3 , $(\text{UO}_2)_2\text{CO}_3(\text{OH})_3^-$, and others are enhanced because the concentrations of dissolved CO_2 increase. The main amounts of strontium in waters are transported in the ionic form [51–53].

The interaction of uranium cations with the surface of layered silicates takes place primarily with the formation of strong surface complexes due to the Si–OH, Al–OH, and Mg–OH groups localized on the side faces of minerals. Sorption isotherms were obtained at neutral pH (pH 6), where the dissociation of the surface groups of the Si(Al)OH groups on the side faces of the mineral particles takes place. The sorption of strontium ions on layered silicates includes two different mechanism: the cation exchange in the interlayers resulting

from the interactions between ions and negative permanent charge and the formation of inner-sphere complexes through Si–O– and Al–O– groups at the clay particle edges [54].

The aforementioned results confirmed that thermal, acid, and mechanochemical treatment significantly changed the structure and morphology of the particles of montmorillonite, which are demonstrated in the general schema (Figure 7).

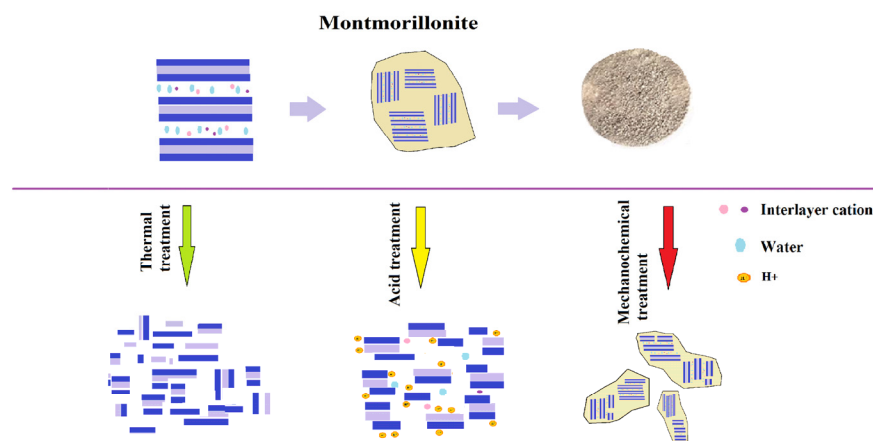


Figure 7. Schematic illustration of the effect of the different methods of montmorillonite treatment: thermal, acid, and mechanochemical.

The values of uranium sorption (Figure 6a, Table 2) correlate with the values of the specific surface area of montmorillonite for all the obtained samples (Table 1). For Sr²⁺ ions (Figure 6b, Table 2), the increase in sorption correlates with the 2 h MCA MMT sample.

During acid activation, the destruction of the crystalline structure of the silicates occurred due to the ion exchange of surface cations for acid protons. At further transformations, H⁺ protons penetrated the hexagonal holes of the tetrahedral networks and attacked the structural cations of the octahedral networks of the mineral. The magnesium octahedra are the most vulnerable to proton attack, whereas the Al³⁺ and Fe³⁺ octahedra are somewhat more resistant to acids. However, they also undergo structural degradation and leaching if the process continues long enough [19]. Acid-activated montmorillonites HNO₃ MMT and HCl MMT were gradually destroyed and replaced by a crystalline structure by the amorphous phase of the silica gel, which was confirmed by the data of the X-ray phase analysis. At the same time, the porosity of the acid-activated montmorillonite changed significantly due to the partial dissolution of its oxide structure. There was an increase in the specific surface from 89.1 to 179.4 and 244.0 m²/g and the volume of pores from 0.078 cm³/g to 0.198 and 0.304 cm³/g. The new mesopores are gaps between the particles of the amorphous silica gel and non-destroyed aluminosilicate layers of the mineral [19,29]. The increase in the uranium sorption values on the acid-activated montmorillonite samples (161.3 and 140.9 μmol/g for HCl MMT and HNO₃ MMT samples, respectively) is due to the appearance of new sorption centers formed by proton attack. However, some negative effects for strontium were observed on acid-treated montmorillonite. The positively charged strontium ions underwent a more difficult reaction with the surface of the sorbent and so decreasing sorption was observed. The first reason for this effect is that the negative charge on the surface of the montmorillonite was partly neutralized by the acid treatment. And the next reason was as a result of the protonation of the Si–OH groups or the acceptance of protons by octahedrally coordinated Al³⁺ or that Fe³⁺ positively charged sites were generated [55].

In the case of layered silicates, due to the low rigidity of their structural frame, even with relatively small exposure energy and exposure time, significant changes occurred. The latter affected not only the specific surface of the material being crushed (increasing from 89.1 m²/g to 146.8 m²/g for 2 h MCA MMT) but also the character of its porous structure, which is also manifested in deeper deformations of the tetrahedral and octahedral meshes

of the elementary aluminosilicate packets. In the process of mechanical activation, the porous structure of the layered silicates undergoes significant changes, with the total pore volume increasing from 0.078 to 0.161 cm³/g. At the same time, the changes concern both the primary porosity, determined by the structure of the minerals themselves, and the secondary porosity in aggregates of clay particles [34–36]. With fine dispersion, the formation of “fluffy” side faces occurs. At the same time, the surface areas easily accessible to the radionuclides in the interlayer space of minerals near the side faces increases, which leads to an increase in their sorption values (from 67.6 to 120.5 for U(VI) and from 434.8 to 555.6 μmol/g and Sr(II) on 2 h MCA MMT) [36,56]. These improvements can be attributed to the increased surface available for adsorption, because of the decrease in the clay particle size, as well as the exfoliation of the clay mineral particles.

For the thermal-treated montmorillonite, the decrease in the sorption values of the uranyl ions from 67.6 to 55.0 μmol/g and strontium ions from 434.0 to 163.9 μmol/g correlated with the decrease in the specific surface (75.4 m²/g). The thermal treatment of the natural MMT leads to a decrease in the mass that is connected with the removal of different forms of bound water. During thermal modification, there is a loss in the ability to interlayer the swelling of the montmorillonite structure, and, thus, a decrease in the size of the active surface, which can participate in ion exchange. The heat treatment of montmorillonite also affects the acidic nature of its surface [40]. The partial thermal removal of interlayer water increases the proton-donating capacity of its molecules. A gradual increase in temperature is accompanied by the transition of silanol groups to siloxane groups with their subsequent irreversible destruction at temperatures >600 °C [41,57]. The main part of the strontium ions, thus, binds on the thermally treated montmorillonite on the side faces of the mineral particles with the formation of strong surface complexes.

5. Conclusions

Thermal, acid, and mechanochemical activation significantly change the structural properties and sorption characteristics of montmorillonite. Various changes in these properties, such as the destruction of the crystalline phase and its transformation into amorphous, the particle size reduction, the domination of spherulitic and (quasi-)regular particles, and the increase in specific surface area and total pore volume, were observed following the treatment of the temperature, acids, and milling.

It was established that the thermal treatment of montmorillonite at 600 °C leads to a collapse followed by the dehydroxylation of the layered sheets. Chemical treatments with HNO₃ or HCl also destroy the mineral structure and the cause the dissolution of the tetrahedrally coordinated Al and Si ions. Mechanochemical activation leads to the partial amorphization of the structure too. The samples of montmorillonite with the obtained physical–chemical characteristics demonstrate high sorption properties to uranium ions. The effective removal of strontium ions can be produced by mechanoactivated montmorillonite.

Thus, sorption materials on a base of thermal-, acid-, and mechanochemical-modified montmorillonite can be used for the removal of radionuclides uranium (VI) and strontium (II) from contaminated water as effective cheap sorbents.

Funding: This research received no external funding.

Institutional Review Board Statement: Not applicable.

Informed Consent Statement: Not applicable.

Data Availability Statement: Not applicable.

Acknowledgments: The author is grateful to the staff of the Institute for Sorption and Problems of Endoecology and the Institute of General and Inorganic Chemistry of the National Academy of Sciences of Ukraine for their help and support in the experiment.

Conflicts of Interest: The author declares no conflict of interest.

References

1. Landa, E.R. Uranium mine tailings: Nuclear waste and natural laboratory for geochemical and radioecological investigations. *J. Environ. Radioact.* **2004**, *77*, 1–27. [[CrossRef](#)] [[PubMed](#)]
2. Chen, Z.; Wang, S.; Hou, H.; Chen, K.; Gao, P.; Zhang, Z.; Jin, Q.; Pan, D.; Guo, Z.; Wu, W. China's progress in radionuclide migration study over the past decade (2010–2021): Sorption, transport and radioactive colloid. *Chin. Chem. Lett.* **2022**, *33*, 3405–3412. [[CrossRef](#)]
3. World Health Organization. *Guidelines for Drinking-Water Quality: Fourth Edition Incorporating the First and Second Addenda*; World Health Organization: Geneva, Switzerland, 2022.
4. Kornilovych, B.Y.; Sorokin, O.G.; Pavlenko, V.M.; Koshyk, Y.I. *Environmental Protection Technologies in the Uranium Mining and Processing Industry*; Norma: Kyiv, Ukraine, 2011; p. 154. (In Ukrainian)
5. Chakraborty, R.; Asthana, A.; Singh, A.K.; Jain, B.; Susan, A.B.H. Adsorption of heavy metal ions by various low-cost adsorbents: A review. *Int. J. Environ. Anal. Chem.* **2020**, *102*, 342–379. [[CrossRef](#)]
6. Jun, B.-M.; Lee, H.-K.; Park, S.; Kim, T.-J. Purification of uranium-contaminated radioactive water by adsorption: A review on adsorbent materials. *Sep. Purif. Technol.* **2022**, *278*, 119675. [[CrossRef](#)]
7. Kravchenko, M.V.; Khodakovska, T.A.; Kovtun, M.F.; Romanova, I.V. Inorganic sorbents based on magnesium silicates obtained by two synthetic routes. *Environ. Earth Sci.* **2022**, *81*, 549. [[CrossRef](#)]
8. Bergaya, F.; Theng, B.K.; Lagaly, G. (Eds.) *Handbook of Clay Science*; Elsevier Ltd.: Amsterdam, The Netherlands, 2006; Volume 1.
9. Komadel, P.; Madejova, J.; Bujdak, J. Preparation and properties of reduced-charge smectites—A review. *Clays Clay Miner.* **2005**, *53*, 313–334. [[CrossRef](#)]
10. Bhattacharyya, K.G.; Gupta, S.S. Adsorption of a few heavy metals on natural and modified kaolinite and montmorillonite: A review. *Adv. Colloid Interface Sci.* **2008**, *140*, 114–131. [[CrossRef](#)]
11. Novikau, R.; Lujaneniene, G. Adsorption behaviour of pollutants: Heavy metals, radionuclides, organic pollutants, on clays and their minerals (raw, modified and treated): A review. *J. Environ. Manag.* **2022**, *309*, 114685. [[CrossRef](#)]
12. Yuan, G.D.; Theng, B.K.G.; Churchman, G.J.; Gates, W.P. Clays and Clay Minerals for Pollution Control. In *Handbook of Clay Sciences*; Elsevier: Amsterdam, The Netherlands, 2013; Volume 5, pp. 587–644.
13. Misaelides, P. Clay minerals and zeolites for radioactive waste immobilization and containment. In *Modified Clay and Zeolite Nanocomposite Materials*; Elsevier: Amsterdam, The Netherlands, 2019; pp. 243–274.
14. Youssef, W.M. Uranium Adsorption from Aqueous Solution Using Sodium Bentonite Activated Clay. *J. Chem. Eng. Process Technol.* **2017**, *8*, 157–170.
15. Tran, E.L.; Teutsch, N.; Klein-BenDavid, O.; Weisbrod, N. Uranium and Cesium sorption to bentonite colloids under carbonate-rich environments: Implications for radionuclide transport. *Sci. Total Environ.* **2018**, *643*, 260–269. [[CrossRef](#)]
16. El-Kamash, A.M. Evaluation of zeolite A for the sorptive removal of Cs⁺ and Sr²⁺ ions from aqueous solutions using batch and fixed bed column operations. *J. Hazard. Mater.* **2008**, *151*, 432–445. [[CrossRef](#)]
17. Tamayo, A.; Kyziol-Komosinska, J.; Sánchez, M.; Calejas, P.; Rubio, J.; Barba, M. Characterization and properties of treated smectites. *J. Eur. Ceram. Soc.* **2012**, *322*, 831–2841. [[CrossRef](#)]
18. Kovalchuk, I. Clay-Based Sorbents for Environmental Protection from Inorganic Pollutants. *Environ. Sci. Proc.* **2023**, *25*, 34. [[CrossRef](#)]
19. Komadel, P.; Madejova, J. Acid activation of clay minerals. In *Handbook of Clay Science*; Elsevier: Amsterdam, The Netherlands, 2013; Volume 5, pp. 385–409.
20. Mucsi, G. A review on mechanical activation and mechanical alloying in stirred media mill. *Chem. Eng. Res. Des.* **2019**, *148*, 460–474. [[CrossRef](#)]
21. Heller-Kallai, L. Thermally modified clay minerals. In *Handbook of Clay Sciences*; Elsevier: Amsterdam, The Netherlands, 2013; Volume 5, pp. 411–433.
22. Kovalchuk, I.A.; Laguta, A.N.; Kornilovych, B.Y.; Tobilko, V.Y. Organophilic layered silicates for sorption removal of uranium(VI) from mine water. *Chem. Phys. Surf. Technol.* **2020**, *2*, 215–227. [[CrossRef](#)]
23. Mnasri-Ghniimi, S.; Frini-Srasra, N. Removal of heavy metals from aqueous solutions by adsorption using single and mixed pillared clays. *Appl. Clay Sci.* **2019**, *179*, 105–151. [[CrossRef](#)]
24. Zhao, X.; Liu, W.; Cai, Z.; Han, B.; Qian, T.; Zhao, D. An overview of preparation and applications of stabilized zero-valent iron nanoparticles for soil and groundwater remediation. *Water Res.* **2016**, *100*, 245–266. [[CrossRef](#)]
25. Kornilovych, B.; Kovalchuk, I.; Tobilko, V.; Ubaldini, S. Uranium Removal from Groundwater and Wastewater Using Clay-Supported Nanoscale Zero-Valent Iron. *Metals* **2020**, *10*, 1421. [[CrossRef](#)]
26. Tobilko, V.Y.; Spasonova, L.M.; Kovalchuk, I.A.; Kornilovych, B.Y.; Kholodko, Y.M. Adsorption of Uranium (VI) from Aqueous Solutions by Amino-functionalized Clay Minerals. *Colloids Interfaces* **2019**, *3*, 41. [[CrossRef](#)]
27. Takahashi, C.; Shirai, T.; Fuji, M. Study on intercalation of ionic liquid into montmorillonite and its property evaluation. *Mater. Chem. Phys.* **2012**, *135*, 681–686. [[CrossRef](#)]
28. Kovalchuk, I.; Tobilko, V.; Kholodko, Y.; Zahorodniuk, N.; Kornilovych, B. Purification of mineralized waters from U(VI) compounds using bentonite/iron oxide composites. *Technol. Audit. Prod. Reserves* **2020**, *3*, 12–18. [[CrossRef](#)]
29. Önal, M.; Sarikaya, Y. Preparation and characterization of acid-activated bentonite powders. *Powder Technol.* **2007**, *172*, 14–18. [[CrossRef](#)]

30. Yassin, J.M.; Shiferaw, Y.; Tedla, A. Application of acid activated natural clays for improving quality of Niger (*Guizotia abyssinica* Cass) oil. *Heliyon* **2022**, *8*, e09241. [[CrossRef](#)] [[PubMed](#)]
31. Bhattacharyya, K.G.; Gupta, S.S. Adsorptive accumulation of Cd(II), Co(II), Cu(II), Pb(II), and Ni(II) from water on montmorillonite: Influence of acid activation. *J. Colloid Interface Sci.* **2007**, *310*, 411–424. [[CrossRef](#)]
32. Gupta, S.S.; Bhattacharyya, K.G. Adsorption of heavy metals on kaolinite and montmorillonite: A review. *Phys. Chem. Chem. Phys.* **2012**, *19*, 6698–6723. [[CrossRef](#)] [[PubMed](#)]
33. Yariv, S.; Lapidés, I. The Effect of Mechanochemical Treatments on Clay Minerals and the Mechanochemical Adsorption of Organic Materials onto Clay Minerals. *J. Mater. Synth. Process.* **2000**, *8*, 223–233. [[CrossRef](#)]
34. Xia, M.; Jiang, Y.; Zhao, L.; Li, F.; Xue, B.; Sun, M.; Liu, D.; Zhang, X. Wet grinding of montmorillonite and its effect on the properties of mesoporous montmorillonite. *Colloids Surf. A Physicochem. Eng. Asp.* **2010**, *356*, 1–9. [[CrossRef](#)]
35. Vdović, N.; Jurina, I.; Škapin, S.D.; Sondi, I. The surface properties of clay minerals modified by intensive dry milling—Revisited. *Appl. Clay Sci.* **2010**, *48*, 575–580. [[CrossRef](#)]
36. Kornilovych, B.Y. *Structure and Surface Properties of Mechanochemically Activated Silicates and Carbonates*; Naukova Dumka: Kyiv, Ukraine, 1994; p. 127. (In Ukrainian)
37. Godet-Morand, L.; Chamayou, A.; Dodds, J. Talc grinding in an opposed air jet mill: Start-up, product quality and production rate optimization. *Powder Technol.* **2002**, *128*, 306–313. [[CrossRef](#)]
38. Djukić, A.; Jovanović, U.; Tuvić, T.; Andrić, V.; Novaković, J.G.; Ivanović, N.; Matović, L. The potential of ball-milled Serbian natural clay for removal of heavy metal contaminants from wastewaters: Simultaneous sorption of Ni, Cr, Cd and Pb ions. *Ceram. Int.* **2013**, *39*, 7173–7178. [[CrossRef](#)]
39. Kumrić, K.R.; Đukić, A.B.; Trtić-Petrović, T.M.; Vukelić, N.S.; Stojanović, Z.; Grbović Novaković, J.D.; Matović, L.L. Simultaneous removal of divalent heavy metals from aqueous solutions using raw and mechanochemically treated interstratified montmorillonite/kaolinite clay. *Ind. Eng. Chem. Res.* **2013**, *52*, 7930–7939. [[CrossRef](#)]
40. Hong, W.; Meng, J.; Li, C.; Yan, S.; He, X.; Fu, G. Effects of Temperature on Structural Properties of Hydrated Montmorillonite: Experimental Study and Molecular Dynamics Simulation. *Adv. Civil Eng.* **2020**, *2020*, 8885215. [[CrossRef](#)]
41. Aytas, S.; Yurtlu, M.; Donat, R. Adsorption characteristic of U(VI) ion onto thermally activated bentonite. *J. Hazard. Mater.* **2009**, *172*, 667–674. [[CrossRef](#)]
42. Tobilko, V.Y.; Kovalchuk, I.A.; Kornilovych, B.Y.; Denisova, T.I.; Kravchenko, O.V. Sorption of uranium and cobalt ions by thermally modified layered silicates. *Rep. Natl. Acad. Sci. Ukr.* **2010**, *5*, 150–155.
43. Espaca, V.A.A.; Sarkar, B.; Biswas, B.; Rusmin, R.; Naidu, R. Environmental applications of thermally modified and acid activated clay minerals: Current status of the art. *Environ. Technol. Innov.* **2019**, *13*, 383–397. [[CrossRef](#)]
44. Brindley, G. *Crystal Structures of Clay Minerals and Their X-ray Identification*; Brown, G., Ed.; The Mineralogical Society of Great Britain and Ireland: London, UK, 1980; p. 496.
45. Rouquerol, F.; Rouquerol, J.; Sing, K.S.W.; Llewellyn, P.; Maurin, G. *Adsorption by Powders and Porous Solids*; Elsevier: Amsterdam, The Netherlands, 2014.
46. Langmuir, I. The adsorption of gases on plane surfaces of glass, mica and platinum. *J. Am. Chem. Soc.* **1918**, *40*, 1361–1403. [[CrossRef](#)]
47. Freundlich, H.; Heller, W. The Adsorption of cis- and trans-Azobenzene. *J. Am. Chem. Soc.* **1939**, *61*, 2228–2230. [[CrossRef](#)]
48. Kovalchuk, I.A.; Spasyonova, L.M.; Zakutevskiy, O.I. Sorptive purification of radioactively contaminated waters by acid and mechanical activation montmorillonite. In Proceedings of the Materials of the Seventh International Conference on Nuclear Decommissioning and Environment Recovery INUDECO 22, Slavutych, Ukraine, 27–28 April 2022.
49. Sun, L.; Liang, X.; Liu, H.; Cao, H.; Liu, X.; Jin, Y.; Li, X.; Chen, S.; Wu, X. Activation of Co-O bond in (110) facet exposed Co₃O₄ by Cu doping for the boost of propane catalytic oxidation. *J. Hazard. Mater.* **2023**, *452*, 131319. [[CrossRef](#)]
50. Feng, X.; Hu, H.; Chen, D. Key nanomaterials for industrial chemical process. *Nano Res.* **2023**, *16*, 6212–6219. [[CrossRef](#)]
51. Merkel, B.J.; Hasche-Berger, A. *Uranium, Mining and Hydrogeology*; Springer: Berlin/Heidelberg, Germany, 2008; p. 955.
52. Liu, B.; Peng, T.; Hong-Juan, S.; Yue, H. Release behavior of uranium in uranium mill tailings under environmental conditions. *J. Environ. Radioact.* **2017**, *171*, 160–168. [[CrossRef](#)]
53. Atwood, D.A. (Ed.) *Radionuclides in the Environment*; Wiley: Hoboken, NJ, USA, 2010; p. 522.
54. Kraepiel, A.M.L.; Keller, K.; Morel, F.M.M. A model for metal adsorption on montmorillonite. *J. Colloid Interface Sci.* **1999**, *210*, 43–54. [[CrossRef](#)] [[PubMed](#)]
55. Pradas, E.G.; Sánchez, M.V.; Cruz, F.C.; Viciana, M.S.; Pérez, M.F. Adsorption of cadmium and zinc from aqueous solution on natural and activated bentonite. *J. Chem. Technol. Biotechnol.* **1994**, *59*, 289–295. [[CrossRef](#)]
56. Bekri-Abbes, I.; Srasra, E. Effect of mechanochemical treatment on structure and electrical properties of montmorillonite. *J. Alloys Compd.* **2016**, *671*, 34–42. [[CrossRef](#)]
57. Gao, Y.; Wang, Y.; Chen, C.; Zhou, J.; Cheng, Y.; Shi, L. Preparation of Montmorillonite Nanosheets with a High Aspect Ratio through Heating/Rehydrating and Gas-Pushing Exfoliation. *Langmuir* **2022**, *38*, 10520–10529. [[CrossRef](#)] [[PubMed](#)]

Disclaimer/Publisher's Note: The statements, opinions and data contained in all publications are solely those of the individual author(s) and contributor(s) and not of MDPI and/or the editor(s). MDPI and/or the editor(s) disclaim responsibility for any injury to people or property resulting from any ideas, methods, instructions or products referred to in the content.